

Douglas K. Miller and Wendell A. Nuss
Naval Postgraduate School, Monterey, California

Patrick S. Cross
U.S. Navy/Submarine Forces/ U.S. Pacific Fleet, Pearl Harbor, Hawaii

1. INTRODUCTION

A low-level core of high wind speeds aligned along the U.S. West Coast, known as the coastal jet, is a persistent feature during the summer months. The seasonal preference for such a feature is a function of several conditions; warm temperatures inland, cool air offshore maintained by coastal upwelling, and a capping inversion at the top of the marine boundary layer forced by subsidence associated with the eastern Pacific sub-tropical high.

Several mechanisms have been proposed to explain the genesis and maintenance of the coastal jet based on several field experiments and modeling studies. Small-scale wind speed maxima observed in the lee of capes and points have led to the hypothesis that supercritical flow is potentially responsible for their formation (Winant et al. 1988). Mountain wave effects have also been proposed (Burk and Thompson 1996) as potentially important contributors in the lifecycle of the coastal jet.

The Naval Postgraduate School (NPS) Real-Time MM5 Forecast System simulations of the coastal jet, with an innermost domain grid spacing of 12 km, show it to be a broad and persistent feature with the low-level wind speed maxima generally located along the coast downstream of capes and points. At such a relatively coarse resolution, it is doubtful that gravity waves associated with supercritical flow are capable of being captured in the simulation. Also, the coastal mountains are not fully resolved so that mountain wave effects are, at best, weaker in the simulations than in reality. Yet, the simulated coastal jet at 12 km grid spacing shows a structure and lifecycle consistent with the observations of field experiments.

The purpose of this study is to investigate simple mechanisms contributing to the development of the coastal jet that are unconstrained by special

*Corresponding author address: Douglas Miller, Department of Meteorology, Naval Postgraduate School, Monterey, CA 93943; email: dkmiller@nps.navy.mil.

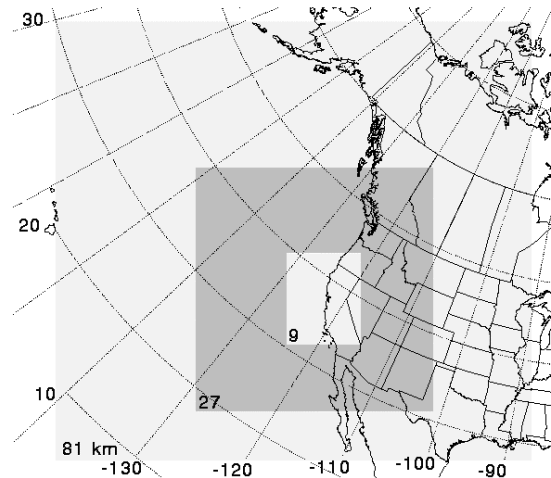


Figure 1: COAMPS nested grid configuration with grid spacings decreasing from 81 to 9 km in multiples of 3.

atmospheric conditions. This work is a follow-on study to that completed by Cross (2003) in which the coastal jet evolution was examined using a mesoscale numerical model.

2. METHODOLOGY

In this study, the full-physics mesoscale model of the U.S. Navy (COAMPSTM) is applied in order to investigate the evolution of the coastal jet. The mesoscale model domain configuration, whose location is shown in Figure 1, consists of three nested domains ranging from 81 to 9 km grid spacing, with a grid spacing ratio of 3 between consecutive domains.

The model top is prescribed to be at 20 km with 47 vertical levels from the surface to model top. Each mesoscale model forecast consists of a 36-h simulation generated using a “cold-start” approach, wherein the initial conditions have been computed using two-dimensional multiquadric univariate interpolation blending available National Weather Service observations with the U.S. Navy Operational Global Atmospheric Prediction System (NOGAPS) model forecast fields for creating initial and lateral boundary conditions of the outermost domain updated every 12 hours.

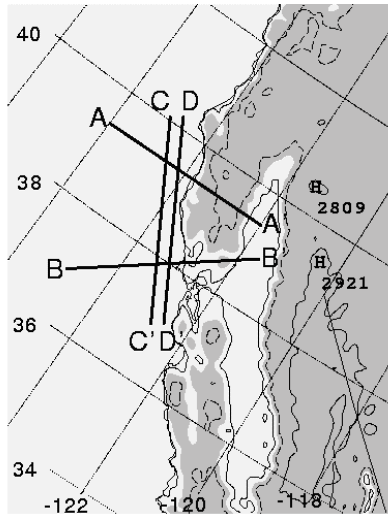


Figure 2: COAMPS 9 km domain terrain elevation (m). Elevations of 100, 2500 (solid), and 1000 m (dash) are contoured and elevations exceeding 500 m are shaded.

One-way nesting is prescribed so that information is communicated through the lateral boundaries of the inner domains from the mother domain.

The 9 km COAMPS™ domain terrain elevation field generated for the simulations (Figure 2) shows the coastal range that forms a wall at Cape Mendocino (near point “D”) and extends to over 1000 m above sea level. The focus of the study will be along the northcentral coast of California, as indicated in Figure 2 by the lines of the cross-coast and along-coast vertical cross sections.

Two numerical experiments will be used to test the impact of local coastal geometry and topography in the development of the coastal jet. The control experiment (CTRL) utilizes the default 9 km gridded topographic, land-use, albedo, and roughness length data files as input. The second experiment (XCST) extends the coastline 5 grid points (45 km) away from the default coastline. The extended coastal zone is forced with an elevation of 2 cm and maintains the land-use, albedo, and roughness length value of the inland coastal grid point from the default experiment.

Two case studies will be examined which occurred during the Coastal Waves 1996 experiment, each differ slightly in the positioning of the coastal surface pressure gradient. Results from the 9 JUN 1996 will be presented here and those of the 14 JUN 1996 case will be given at the oral presentation.

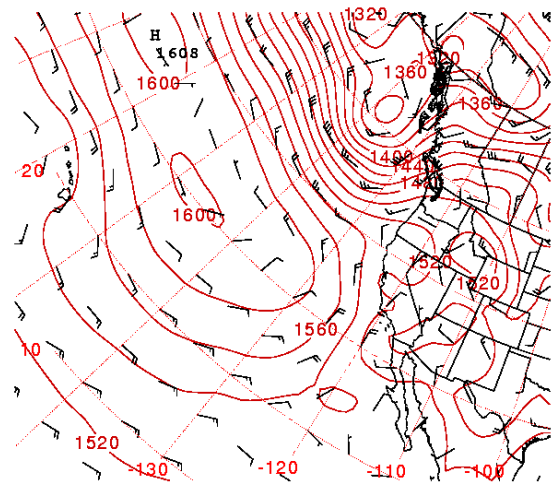


Figure 3: NOGAPS geopotential height (m, contours) and winds (knots) at the 850 hPa level valid 0000 UTC 9 JUN 1996.

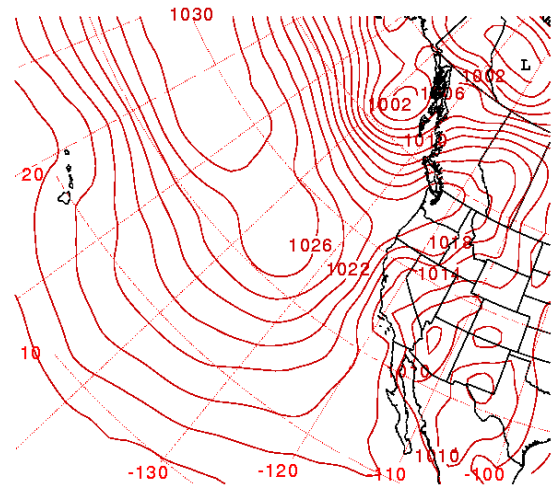


Figure 4: NOGAPS mean sea level pressure (hPa, contours) valid 0000 UTC 9 JUN 1996.

The synoptic pattern as derived from the U.S. Navy NOGAPS valid 0000 UTC 9 JUN (Figures 3 and 4) shows the eastern North Pacific high at the 850 hPa (Fig. 3) and sea (Fig. 4) levels. The ridge axis is aligned from southwest to northeast, with the axis crossing the coast near Cape Mendocino. Winds at the 850 hPa level show northwesterly flow along the coast. Observations from the Coastal Waves 1996 experiment indicated the presence of a significant coastal jet on this day (not shown).

3. NUMERICAL RESULTS

The simulated 27-h 1000 hPa level isotachs and 850 hPa level winds for the CTRL (Fig. 5) and XCST (Fig. 6) experiments each indicate a broad expanse of low-level winds exceeding 10 m s^{-1}

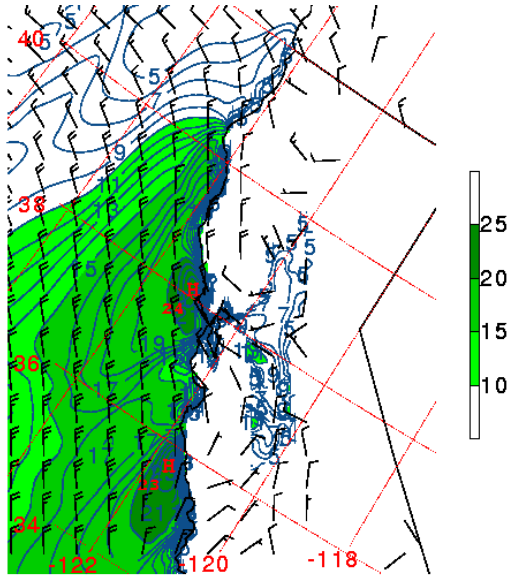


Figure 5: Simulated CTRL 1000 hPa isotachs ($m s^{-1}$, contours and shading) and winds valid 0300 UTC 10 JUN 1996.

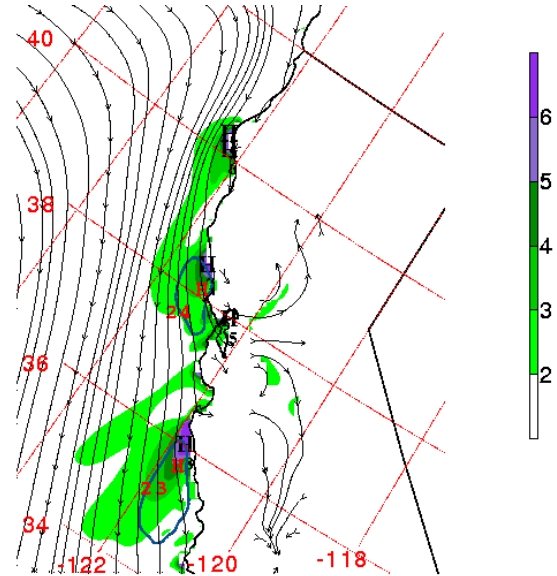


Figure 7: Simulated CTRL 1000 hPa $20 m s^{-1}$ isotach (contour), streamlines, and 1000-700 hPa thickness gradient magnitude ($\times 10^3$, shading) valid 0300 UTC 10 JUN 1996.

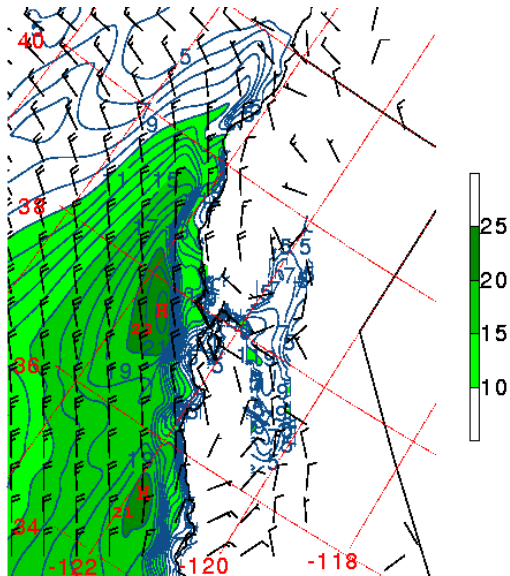


Figure 6: As in Figure 5, except for XCST simulation.

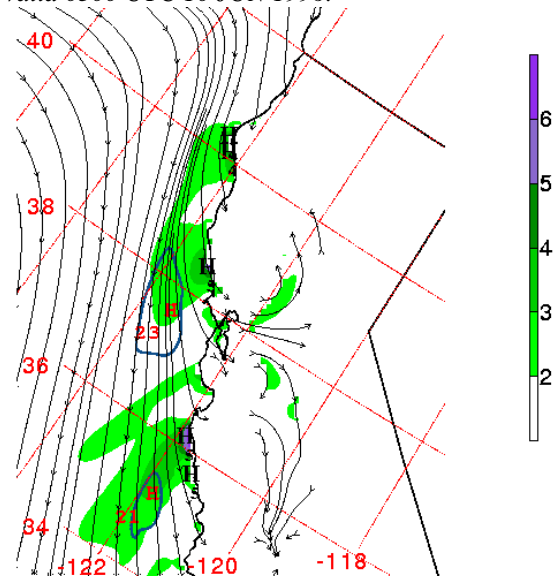


Figure 8: As in Figure 7, except for XCST simulation.

along the central California coast. The impact of the extended coastal zone is evident in the depressed wind speeds in Fig. 6. The wind speed maximum near $38^{\circ}N$ is 24 and $23 m s^{-1}$ in the CTRL and XCST experiments, respectively. The location of the XCST maximum is far enough away from the coastal mountains so that supercritical flow and mountain wave effects cannot be the source of the simulated coastal jet.

plotted with the 1000-700 hPa thickness gradient magnitude in Figures 7 and 8 show a close correspondence between the coastal jet and enhanced low-level baroclinic zones. In both cases, the coastal jet is downstream of the axis of maximum baroclinity. The locations of the enhanced low-level baroclinic zones suggest that coastal geometry and topography plays a role in their existence.

The 1000 hPa streamlines and $20 m s^{-1}$ isotach

Simulated 1000 hPa horizontal divergence for the

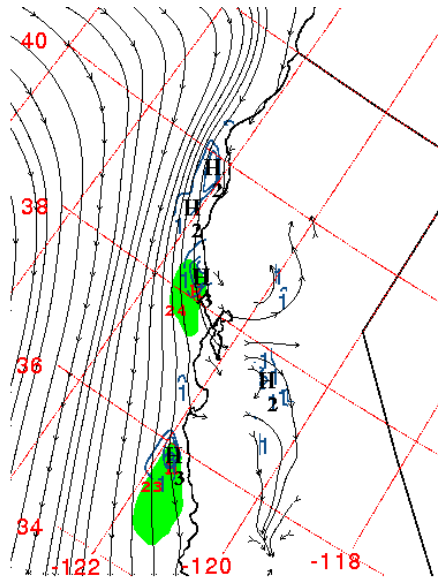


Figure 9: Simulated CTRL 1000 hPa wind speed exceeding 20 m s^{-1} (shading), streamlines, and horizontal divergence ($\times 10^{-5} \text{ s}^{-1}$, contours) valid 0300 UTC 10 JUN 1996.

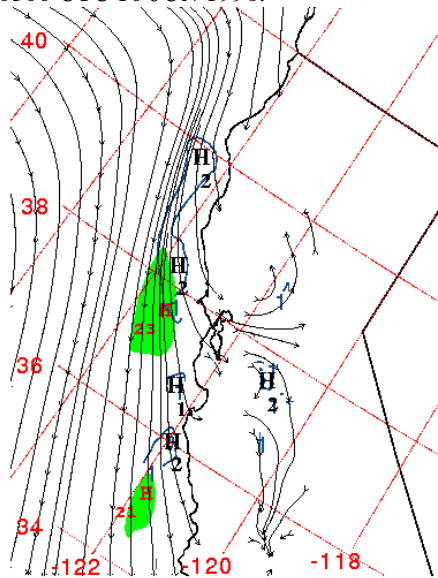


Figure 10: As in Figure 9, except for XCST simulation.

experiments shown in Figures 9 and 10 show a close correspondence between locations of the coastal jet and low-level divergence, with the jet found downstream of the center of divergence. The centers of divergence are fixed along the coastline, downstream of capes and points, as seen in the XCST plot (Fig. 10), and are not tied to coastal topography.

Low-level divergence requires compensating downward motion resulting in an increased slope in

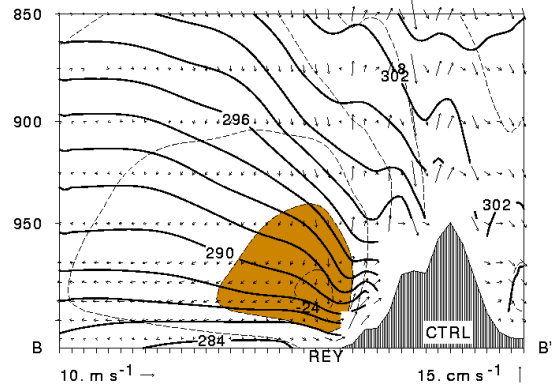


Figure 11: Simulated CTRL cross-coast section B-B' (position given in Fig. 2) of isentropes (solid), isotachs (m s^{-1} , dashed), and wind speed exceeding 20 m s^{-1} (shading) valid 0300 UTC 10 JUN 1996.

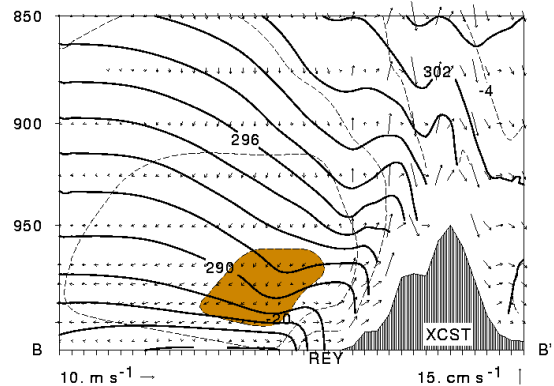


Figure 12: As in Figure 11, except for XCST simulation.

the coastal isentropes and an increased low-level baroclinic zone, as evident in the cross-coast sections shown in Figures 11 and 12. Note the positioning of the coastal jet and the isentropes of greatest slope along the coast in both experiments.

4. REFERENCES

Burk, S.D., and W.T. Thompson, 1996: The summertime low-level jet and marine boundary layer structure along the California coast. *Monthly Weather Review*, **124**, 668-686.

Cross, P.S., 2003: The California coast jet: Synoptic controls and topographically induced mesoscale circulation. Ph.D. Dissertation, Naval Postgraduate School, Monterey, CA, 173 pp.

Winant, C.D., C.E. Dorman, C.A. Friehe, and R.C. Beardsley, 1988: The marine layer of northern California: An example of supercritical channel flow. *Journal of Atmospheric Sciences*, **45**, 3588-3605.